ISSN 1807-1929
Revista Brasileira de Engenharia Agrícola e Ambiental
Brazilian Journal of Agricultural and Environmental Engineering
v.30, n.4, e297188, 2026
Campina Grande, PB – http://www.agriambi.com.br – http://www.scielo.br/rbeaa

Original Article

Kinetic modeling of physiological and quality changes in Cavendish bananas during natural ripening[1]

Modelagem cinética das alterações fisiológicas e de qualidade em bananas Cavendish durante o amadurecimento natural

Rima Kumalasari[2], Andriati Ningrum[3], Achmat Sarifudin[2] & Djagal Wiseso Marseno[3*]

[1] Research developed at Badan Riset dan Inovasi Nasional (BRIN – National Research and Innovation Agency), Subang, West Java, Indonesia
[2] Research Center for Food Technology and Processing, Badan Riset dan Inovasi Nasional, Cibinong, West Java, Indonesia
[3] Department of Food and Agricultural Product Technology/Faculty of Agricultural Technology/Universitas Gadjah Mada, Yogyakarta, Daerah Istimewa Yogyakarta, Indonesia

HIGHLIGHTS:

CO_2 production peaked at stage 6 and showed the strongest correlation with ripening progression.
Firmness declined earlier than visible peel color, confirming its role as a primary indicator of internal ripening.
Peel color and firmness fit logistic models, while respiration and ethylene followed Michaelis-Menten without inhibition.

ABSTRACT: Cavendish bananas undergo marked physiological and quality transformations during natural ripening. This study characterized the kinetics of respiration, ethylene production, peel color, and texture using four mathematical models: zero-order, first-order, logistic, and Michaelis-Menten to determine the best fit. Fruits were stored at ambient conditions (20 ± 2 °C, 80% RH) and evaluated daily across seven ripening stages (S1-S7) with three biological replicates. The results showed a significant increase in CO_2 production, rising by over 400%, accompanied by a 223% increase in O_2 consumption. Both CO_2 and ethylene peaked at Stage 6, with ethylene reaching 466.32 ± 168.65 mL kg^{-1} h^{-1}. Peel color indices (L^*, a^*, b^*, and C^*) increased by 46.88, 173.65, 61.27, and 53.58%, respectively, while °hue, peel stiffness, and pulp firmness declined by 26.4, 66.57, and 79.39%, respectively. Firmness loss occurred earlier than visible peel color changes, and strong correlations were observed between CO_2 production and both color transition and texture softening. Among the tested models, the logistic function best described peel color and firmness (R^2 = 0.92-0.99; RMSE = 1.12-28.83), while the Michaelis-Menten model without inhibition accurately captured respiration and ethylene kinetics (R^2 = 0.96-0.98; RMSE = 0.002-30.48). The findings provide a robust predictive framework for the natural ripening process, offering valuable insights for optimizing postharvest management, improving shelf-life prediction, and reducing losses in Cavendish banana supply chains.

Key words: postharvest physiology, respiration, ethylene, kinetic modeling, quality attributes

RESUMO: As bananas Cavendish passam por transformações fisiológicas e de qualidade acentuadas durante o amadurecimento natural. Este estudo caracterizou a cinética da respiração, produção de etileno, cor da casca e textura, utilizando quatro modelos matemáticos: ordem zero, primeira ordem, logístico e Michaelis-Menten, para determinar o melhor ajuste. Os frutos foram armazenados em condições ambientes (20 ± 2 °C, 80% UR) e avaliados diariamente ao longo de sete estágios de amadurecimento (S1-S7), com três repetições biológicas. Os resultados mostraram um aumento significativo na produção de CO_2, elevando-se em mais de 400%, acompanhado por um aumento de 223% no consumo de O_2. Tanto o CO_2 quanto o etileno atingiram o pico no Estágio 6, com o etileno alcançando 466,32 ± 168,65 mL kg^{-1} h^{-1}. Os índices de cor da casca (L, *a*, b* e C*) aumentaram 46,88; 173,65; 61,27 e 53,58%, respectivamente, enquanto o ângulo de cor (°hue), a rigidez da casca e a firmeza da polpa diminuíram 26,4; 66,57 e 79,39%, respectivamente. A perda de firmeza ocorreu antes das mudanças visíveis na cor da casca, e fortes correlações foram observadas entre a produção de CO_2 e tanto a transição de cor quanto o amolecimento da textura. Entre os modelos testados, a função logística descreveu melhor a cor da casca e a firmeza (R^2 = 0,92-0,99; RMSE = 1,12-28,83), enquanto o modelo de Michaelis-Menten sem inibição capturou com precisão a cinética respiratória e de etileno (R^2 = 0,96-0,98; RMSE = 0,002-30,48). Os resultados fornecem uma estrutura preditiva robusta para o processo de amadurecimento natural, oferecendo insights valiosos para otimizar o manejo pós-colheita, melhorar a previsão da vida útil e reduzir perdas nas cadeias de suprimentos de bananas Cavendish.

Palavras-chave: fisiologia pós-colheita, respiração, etileno, modelagem cinética, atributos de qualidade

• Ref. 297188 – Received 26 May, 2025
* Corresponding author - E-mail: djagal@ugm.ac.id
• Accepted 09 Nov, 2025 • Published 16 Jan, 2026
Editors: Antônio Gustavo de Luna Souto & Hans Raj Gheyi

This is an open-access article distributed under the Creative Commons Attribution 4.0 International License.

Introduction

Cavendish bananas (*Musa acuminata* [AAA Group]) are among the most widely cultivated and consumed banana varieties worldwide, playing a vital role in both national and international trade (Scott, 2021). They account for more than 50% of global banana production, with India, the Philippines, Ecuador, and Indonesia as the leading producers, highlighting the global relevance of this cultivar and the importance of investigating its ripening physiology (Acevedo et al., 2021; Sugianti et al., 2022). As a climacteric fruit, the physiological ripening of the Cavendish bananas is characterized by a distinct surge in respiration and ethylene production. The increase in ethylene production follows a biphasic pattern, with an initial sharp rise during the climacteric phase, followed by a tapering peak (Cordenunsi-Lysenko et al., 2019). The general physiological changes of climacteric fruits are well understood. However, the detailed time-based quantification of respiration and ethylene kinetics of Cavendish bananas under natural ripening remains limited.

Ethylene acts as a powerful signal during fruit ripening, activating a cascade of enzymatic processes that drive key ripening events (Tipu & Sherif, 2024). Hydrolase enzymes begin to degrade cell wall components, resulting in fruit softening (Verma et al., 2015; Kaur et al., 2024). Simultaneously, chlorophyll degradation in the peel results in a visible transition from green to yellow (Müller & Kräutler, 2011). Despite these known processes, most mechanistic studies have relied on exogenous ethylene treatments (Sugianti et al., 2022). This treatment accelerates ripening but may not accurately reflect the more gradual, complex dynamics of natural ripening. The sensory attributes, texture, and color changes are most apparent and play a key role in determining fruit quality and consumer acceptability (Hoppu et al., 2021). Softening results from pectin and hemicellulose breakdown (Paniagua et al., 2014; Shi et al., 2022) while the shift to a vibrant yellow strongly influences purchase decisions (Kapoor et al., 2022). However, limited work has linked these physical changes to physiological variables such as respiration and ethylene during natural ripening.

A kinetic understanding of ripening is vital for predicting shelf-life and optimizing postharvest handling. While logistic models aptly describe sigmoidal changes in color and firmness loss, the Michaelis-Menten equation captures the enzyme-limited kinetics of respiration and ethylene production (Tuly et al., 2023; Xu & Liu, 2024). Such models enable predictive, rather than merely descriptive, analysis for quality management. However, their application has been confined mainly to single parameters in artificially ripened fruit (Sugianti et al., 2022), leaving the integrated kinetics of natural ripening poorly characterized.

This study, therefore, aimed to comprehensively model the natural ripening of Cavendish bananas by evaluating respiration, ethylene, color, and texture using zero-order, first-order, logistic, and Michaelis-Menten models. We hypothesized that model performance would vary across quality attributes. The resulting framework provides a predictive tool to improve supply chain management and reduce losses in systems that rely on natural ripening.

Material and Methods

This research was conducted in 2024 at the Laboratory for Agricultural Product Storage and Product Testing, located at Badan Riset dan Inovasi Nasional (BRIN) in Subang, West Java, Indonesia. This study used giant Cavendish bananas (*Musa acuminata* [AAA Group] 'Giant Cavendish') harvested at 85 days post-flowering, sourced from an orchard in Cigasong-Majalengka Regency, West Java, Indonesia. The site is located at 6.82° S, 108.28° E, 141 m above sea level. The region has a tropical monsoon climate, with an annual average temperature of 26-30 °C, relative humidity of 70-85%, and total rainfall of 2000-2500 mm. Figure 1 presents a map of the Cavendish banana orchard where the samples for this study were collected.

After harvest, the bananas were removed from the bunch and carefully sorted to exclude any showing signs of damage or physical defects. The individual fingers were then separated from the hands, placed into thin-walled polypropylene containers (19 × 16 × 7 cm), with five bananas per container. Each container was covered with a lid perforated with small holes at each corner and in the center, allowing gas exchange while maintaining a semi-closed environment. The samples were stored in an environmental chamber KCL 2000A (Eyela, Tokyo, Japan) under controlled conditions (20 ± 2 °C, 80% relative humidity) and allowed to ripen naturally without any chemical treatment.

The study was arranged in a completely randomized design with a single factor, namely banana ripening stages (S1 to S7), each replicated three times. In each repetition, five individual fruits were evaluated, resulting in a total of 15 fruits per stage. Ripening was monitored across seven stages (S1-S7). These stages were defined according to the internationally recognized Banana Ripening Index (RRI) based on peel color: S1 = full green; S2 = green with a trace of yellow; S3 = more green than yellow; S4 = more yellow than green; S5 = yellow with green tip; S6 = full yellow; and S7 = yellow with brown spots. The samples were stored starting from day 0 after harvest and observed until they reached the ripening stage 7. On average, the stages were reached at the following days postharvest: S1 (0 days), S2 (2 days), S3 (4 days), S4 (5 days), S5 (6 days), S6 (7 days), and S7 (11 days). The progression of ripening stages did not always correspond linearly with observation days, since stage determination was based on RRI values (a^* and peel spotting)

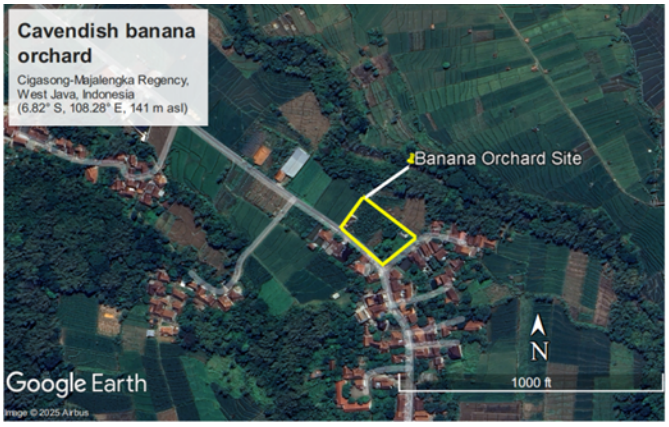

Source - Google Earth Pro, 2025

Figure 1. Location of the Cavendish banana orchard in Cigasong-Majalengka Regency, West Java, Indonesia

rather than the number of days after harvest. This reflects the natural variability of ripening among fruits under ambient conditions. Visual observations were conducted daily, focusing on peel color transition, and samples were collected and analyzed at each noticeable stage of ripening.

Respiration and ethylene production were assessed at each ripening stage using a hermetic respiration chamber connected to a Three Gas Analyzer F-950 (Felix Instruments, USA) (Mendoza et al., 2016). Banana samples were sealed in the chamber for 3 hours before gas concentrations were measured. The fruit samples used were physiologically mature at harvest. The individual fingers had an average weight of 130-150 g, a length of 13-15 cm, a diameter of 30-40 mm, and a volume of 135-150 cm^3. The initial peel color index (a^*) ranged from -10 to -12, confirming full green maturity. The initial flesh firmness was 700-720 gf (equivalent to approximately 6.9-7.1 N). These comprehensive descriptors provide essential baseline information on the biomaterial used in this study. The rates of CO_2 production and O_2 consumption were calculated using the following Eq. 1:

$$R = \frac{V}{W}\frac{dx}{dt} \quad (1)$$

where:

R - respiration or ethylene rate (mL kg^{-1} h^{-1});

x - gas concentration (decimal);

t - time (hours);

V - volume of the chamber (mL); and,

W - weight of sample (kg).

Peel color was measured using a Minolta CR-410 chromameter (Konica Minolta, Osaka, Japan), calibrated with standard black and white tiles. The device recorded L^* (lightness), a^* (red-green), and b^* (yellow-blue) values. Readings were taken at the top, middle, and bottom of each banana and averaged. Chroma (C^*) representing color saturation, and hue angle (hue°) were calculated to better represent color intensity, and dominant hue during ripening was calculated as Eqs. 2 and 3:

$$C^* = \sqrt{a^2 + b^2} \quad (2)$$

$$^{\circ}\text{hue} = \arctan\frac{b}{a} \quad (3)$$

Texture (flesh firmness and peel stiffness) was determined using a texture analyzer. A TA.XT2 Texture Analyzer equipped with a P/2 cylindrical stainless-steel probe (Stable Micro Systems, Surrey, UK) was used. The probe penetrated 10 mm into the fruit at a speed of 0.5 mm s^{-1}, with pre-test and post-test speeds of 1 mm s^{-1} and 10 mm s^{-1}, respectively. The measurements were taken on whole fruits with the peel intact. Peel stiffness was derived from the slope of the force-time curve (g s^{-1}), while flesh firmness was recorded as the maximum penetration force (gf). Readings were taken at three points (top, middle, and bottom) on each banana and averaged.

To describe the dynamic changes in physiological and physical attributes during natural ripening, several mathematical models were tested, including zero-order, first-order, logistic, and Michaelis-Menten equations (with and without inhibition). The general formulations and their applications are summarized in Table 1.

These models were subsequently fitted to experimental data for respiration rate, ethylene production, peel color indices, and textural attributes. Model performance was evaluated using the coefficient of determination (R^2) and root mean square error (RMSE), allowing identification of the most suitable equation to describe ripening-related changes in Cavendish bananas.

Statistical differences among ripening stages were analyzed using one-way ANOVA followed by Duncan's multiple range test ($p \leq 0.05$). Pearson correlation and Principal Component Analysis (PCA) were used to explore relationships among variables. Model performance was evaluated using the RMSE and the coefficient of determination (R^2).

Table 1. Kinetic models used in the study to describe the physiological and physical changes of Cavendish bananas during natural ripening

Model	General Equation	Equation
Zero-Order	$Ct = Co + kt$	(4)
First-Order	$Ct = Co \times e^{-kt}$	(5)
Logistic	$Ct = Uo + \frac{U}{1+\exp[-k(t-to)]}$	(6)
Michaelis–Menten without inhibition	$R = \frac{vm \times YO_2}{km + YO_2}$	(7)
Michaelis–Menten with competitive inhibition	$R = \frac{vm \times YO_2}{km + \left[\left(\frac{YCO_2}{kc}\right) + YO_2\right]}$	(8)
Michaelis–Menten with uncompetitive inhibition	$R = \frac{vm \times YO_2}{km + \left[\left(\frac{YCO_2}{ku}\right) \times YO_2\right]}$	(9)
Michaelis–Menten with noncompetitive inhibition	$R = \frac{vm \times YO_2}{(km + YO_2) \times \left[1 + \left(\frac{YCO_2}{kn}\right)\right]}$	(10)

C_t - Compound concentration at time t; C_0/U_0 - Initial concentration; k: Rate constant; U - The maximum or equilibrium value; t_0 - Midpoint (time when the rate of change is maximal); R - Reaction rate (CO_2, O_2, or ethylene); vm - Maximum rate; y - Substrate concentration (O_2 in this case); km - Michaelis-Menten constant; kc - The carbon dioxide (CO_2) competitive inhibition constant; ku - The CO_2 uncompetitive inhibition constant; kn - The CO_2 noncompetitive inhibition constant

The RMSE was calculated using Eq. 11:

$$RMSE = \sqrt{\frac{\sum_{i=1}^{n}(\hat{y}i - yi)^2}{n}} \quad (11)$$

where:

$\hat{y}i$ - the predicted value from the model at time i;

yi - the actual experimental value at the same time;

i - the observation time, and;

n - the total number of observations.

All data were normalized (Shapiro-Wilk test) before statistical and multivariate analysis to ensure comparability among parameters with different scales. All analyses were performed using SPSS 26, Origin Pro 9.7, and Microsoft Excel 2021.

Results and Discussion

The physiological changes, such as CO_2 production, O_2 consumption, and ethylene emission, along with the

physical changes, including color transformation and texture degradation in Cavendish bananas during natural ripening, are comprehensively presented in Table 2. At the onset of storage, the CO_2 production rate was relatively low, averaging 9.93 ± 0.01 mL kg^{-1} h^{-1}. As the fruit progressed through stages 3 and 4, this rate increased sharply (by more than 400%), peaking at 52.33 ± 5.60 mL kg^{-1} h^{-1} during stage 6. A similar pattern was observed in O_2 consumption, which rose from 18.13 ± 2.05 to 62.24 ± 11.04 mL kg^{-1} h^{-1} before declining in stage 7 (Table 2). The result also showed that the ethylene production was initially undetectable. It began to rise at stage 3 (2.23 ± 0.38 mL kg^{-1} h^{-1}), increased almost 420% by stage 4, and reached its peak at stage 6 (466.32 ± 168.65 mL kg^{-1} h^{-1}) before declining to 165.63 ± 8.09 mL kg^{-1} h^{-1} in the overripe phase (Table 2).

The decline in ethylene production at stage 7 may be attributed to tissue senescence, reduced metabolic activity, and degradation of ethylene biosynthetic enzymes, which collectively limit further hormone synthesis during the late phase of ripening (Tipu & Sherif, 2024). This rise and fall is typical of the climacteric phase, driven by elevated energy demand for ripening-related biosynthetic activities (Nambi et al., 2016). The "ethylene burst" is triggered by the up-regulation of ACC synthase and ACC oxidase, the two key enzymes of ethylene biosynthesis, and occurs in an autocatalytic manner (Tipu & Sherif, 2024). This surge triggers a cascade of ripening responses, including softening, starch degradation, pigment conversion, and volatile production (Verma et al., 2015).

Ethylene acts upstream of respiration to meet the metabolic demands of ripening (Mendoza et al., 2016). Compared to artificially ripened bananas, which reach ethylene peaks within 24-48 h, the natural ripening profile progressed more gradually, with the climacteric peak occurring on days 6-7. This slower pace favors uniform enzymatic activity, enhanced flavor compound formation, and improved textural integrity traits associated with superior eating quality (Cordenunsi-Lysenko et al., 2019; Tipu & Sherif, 2024). Understanding these physiological dynamics is essential for optimizing postharvest management without relying on exogenous ripening agents.

Color transformation in banana peel is among the most prominent visual indicators of ripening, directly reflecting internal metabolic changes and pigment transitions (Table 3). Significant color evolution was observed across all seven ripening stages. The transition from green to yellow was marked by a dramatic shift in a^* values from -11.46 ± 0.23 (Stage 1) to 8.44 ± 0.16 (Stage 7), indicating a complete loss of greenness and the emergence of red-yellow hues. Concurrently, lightness (L^*) increased from 47.34 ± 0.98 to 69.54 ± 0.39, while yellowness (b^*) rose from 31.50 ± 1.04 to 50.80 ± 0.16, resulting in a 53.58% increase in color intensity (C^*). A stage-specific analysis revealed that the most critical color changes occurred between Stages 4 and 6. During this period, the a^* value shifted from negative to positive, indicating rapid chlorophyll degradation and the unmasking of carotenoids. The b^* and C^* values also peaked at Stage 6, corresponding to the fruit's visually vibrant yellow appearance. By Stage 7, a slight decline in C^* suggested the initial onset of peel senescence, characterized by a dulling of color intensity, with chlorophyll degradation complete and carotenoids beginning to oxidize. In parallel, hue angle (hue°) values decreased steadily from ~110° (green) to ~80° (yellow), with intermediate values (~90-100°) clearly distinguishing the transition stage. This pattern provides a more integrative color parameter, capturing the overall shift in peel hue and reinforcing its usefulness as an objective ripening index. These trends are consistent with previous reports on Cavendish and other climacteric fruits, where peel yellowing is driven by chlorophyll degradation and carotenoid accumulation (Müller & Kräutler, 2011; Kapoor et al., 2022).

Figure 2 illustrates the visual transition of Cavendish bananas across ripening stages. The progression from green

Table 2. Physiological changes of Cavendish bananas during natural ripening

Ripening stages	Storage time (DAH)	CO_2 production	O_2 consumption	Ethylene production
		(mL kg^{-1} h^{-1})		
Stage 1	0	9.93 ± 0.01^{a*}	19.26 ± 0.55^{a}	0 ± 0^{a}
Stage 2	2	9.05 ± 0.85^{a}	18.13 ± 2.05^{a}	0 ± 0^{a}
Stage 3	4	28.03 ± 2.97^{b}	47.63 ± 5.5^{b}	2.23 ± 0.38^{a}
Stage 4	5	35.41 ± 2.77b^{c}	53.83 ± 0.76^{bc}	11.57 ± 1.07^{ab}
Stage 5	6	40.38 ±3.22^{c}	55.25 ± 4.53^{bc}	93.03 ± 3.16^{ab}
Stage 6	7	52.33 ±5.60^{d}	62.24 ± 11.04^{c}	466.32 ± 168.65^{d}
Stage 7	11	42.85 ± 18.22^{cd}	45.89 ± 4.64^{b}	165.63 ± 8.09^{c}

* Data are presented as mean ± standard deviation (n = 3). Different superscript letters within a column indicate significant differences at $p \leq 0.05$ according to Duncan's test. DAH - Days after harvest

Table 3. Physical changes of Cavendish bananas during natural ripening

Ripening stages	Storage time (DAH)	L^*	a^*	b^*	C^*	hue°	Peel stiffness (g s^{-1})	Flesh firmness (gf)
Stage 1	0	47.34 ± 0.98^{a*}	-11.46 ± 0.23^{a}	31.50 ± 1.04^{a}	33.52 ± 0.90^{a}	110.01 ± 0.99^{g}	2.48 ± 0.01^{d}	715.48 ± 6.12^{g}
Stage 2	2	57.93 ± 1.37^{b}	-8.26 ± 0.19^{b}	36.43 ± 0.47^{b}	37.35 ± 0.51^{b}	102.78 ± 0.13^{f}	2.33 ± 0.46^{c}	702.67 ± 38.41^{f}
Stage 3	4	61.18 ± 0.29^{c}	-7.36 ± 0.31^{c}	37.84 ± 0.57^{b}	38.55 ± 0.62^{b}	101.0 ± 0.29^{e}	2.5 ± 0.07^{d}	637.60 ± 14.46^{e}
Stage 4	5	61.76 ± 0.22^{c}	-5.60 ± 0.27^{d}	42.74 ± 1.26^{c}	43.11 ± 1.21^{c}	97.48 ± 0.57^{d}	3.03 ± 0.41^{b}	398.45 ± 28.53^{d}
Stage 5	6	68.44 ± 0.13^{d}	3.20 ± 0.18^{e}	44.25 ± 0.12^{c}	44.37 ± 0.11^{c}	85.87 ± 0.24^{c}	3.48 ± 0.15^{a}	262.70 ± 40.76^{c}
Stage 6	7	68.62 ± 0.10^{d}	5.66 ± 0.36^{f}	50.06 ± 0.17^{d}	50.38 ± 0.21^{d}	83.55 ± 0.39^{b}	3.67 ± 0.31^{a}	248.96 ± 10.83^{b}
Stage 7	11	69.54 ± 0.39^{d}	8.44 ± 0.16^{g}	50.80 ± 0.16^{d}	51.48 ± 0.44^{d}	80.57 ± 0.10^{a}	0.83 ± 0.23^{a}	147.47 ± 4.09^{a}

* Data are presented as mean ± standard deviation (n = 3). Different superscript letters within a column indicate significant differences at $p \leq 0.05$ according to Duncan's test. DAH - Days after harvest. L^* - Lightness (0 = dark, 100 = light); a^* - Green (-) to red (+); b^* - Blue (-) to yellow (+); C^* - Chroma (0 = neutral gray, higher values = greater color saturation); hue° - Hue angle (~100-120° = green, ~90-100° = greenish-yellow, ~70-90° = yellow)

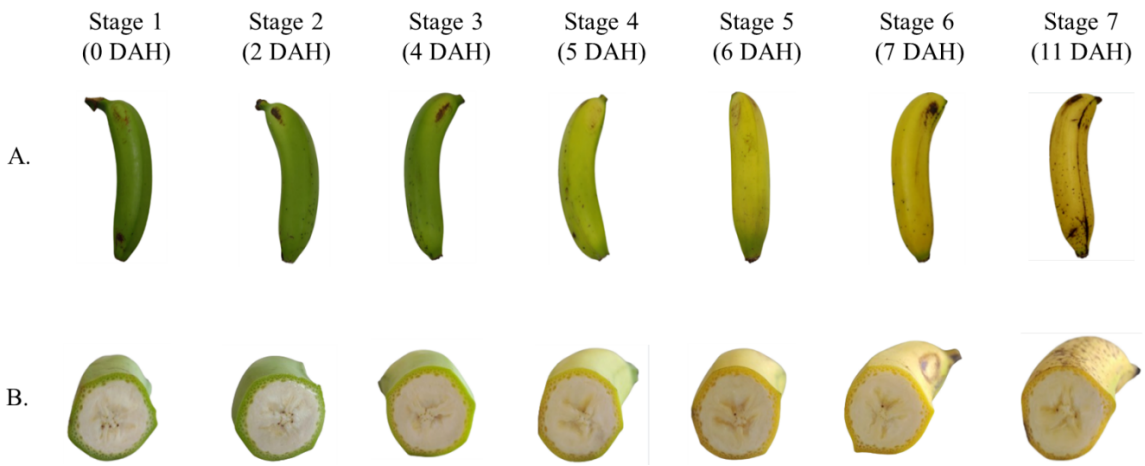

DAH - Days after harvest

Figure 2. Peel color (A) and Cross-section (B) changes in Cavendish bananas during the natural ripening process

(Stage 1-2) to full yellow (Stage 6-7) was consistent with the measured pigment dynamics, where chlorophyll degradation coincided with carotenoid accumulation. The initial green color of banana peel is due to high chlorophyll content, which gradually degrades through a tightly regulated enzymatic pathway. This pathway involves several key enzymes: chlorophyllase, which removes the phytol chain; magnesium dechelatase, which detaches Mg^{2+}; and pheophorbide a oxygenase, which opens the porphyrin ring, converting chlorophyll into fluorescent and non-fluorescent chlorophyll catabolites (Hu et al., 2021; Salaemae et al., 2024).

Chlorophyll breaks down into various compounds, including fluorescent and non-fluorescent catabolites. Fluorescent chlorophyll catabolites (FCCs) can still emit light, even after the original chlorophyll molecules have degraded (Tanaka & Ito, 2025). In contrast, non-fluorescent chlorophyll catabolites no longer fluoresce and are considered more stable end products of this process (Tanaka & Ito, 2025). FCCs are often used as indicators to detect and measure chlorophyll breakdown. Although such catabolites and enzymatic activities were not analyzed in this study, previous research has reported these mechanisms as part of the chlorophyll degradation pathway. Simultaneously, chlorophyll degradation unmasks and promotes the biosynthesis of carotenoids, such as lutein and β-carotene, which impart yellow to orange coloration (Kapoor et al., 2022). According to previous studies, genes such as phytoene synthase and phytoene desaturase, which are essential for carotenoid biosynthesis, are transcriptionally upregulated during ripening in response to ethylene (Shi et al., 2022). This biosynthetic push, alongside chlorophyll breakdown, amplifies the yellow hue that consumers associate with ripeness (Kapoor et al., 2022). These reactions are activated by ethylene signaling, linking hormonal activity with visible pigment changes (Tipu & Sherif, 2024).

The peak rate of color change in this study occurred between Stages 3 and 6 (Figure 2), aligning with the climacteric rise in respiration and ethylene production (Table 2). As shown in Table 2, this transition coincided with significant increases in CO_2 and ethylene production, confirming the tight linkage between pigment turnover and respiratory activity. These physiological processes provide the energy and signaling necessary for pigment turnover. In particular, the a^* value (a sensitive indicator of the green-to-red balance) showed the fastest kinetic change (173.65%), highlighting its utility as a predictive marker of the ripening stage.

Unlike exogenous ethylene treatment, which accelerates ripening and often leads to uneven color development, premature browning, and poor synchronization of pulp texture (Shi et al., 2022). Natural ripening allows gradual and coordinated pigment metabolism. For instance, ethylene-treated bananas can achieve full yellowness within 2-3 days, CO_2 production increased by 387.97% and ethylene by 800% within the first two days (Muthal et al., 2019). In contrast, the climacteric peak in this study occurred on days 6-7. During this peak, CO_2 production rose from 9.93 to 52.33 mL kg^{-1} h^{-1} (an increase of 427.0%), and O_2 consumption rose from 19.26 to 62.24 mL kg^{-1} h^{-1} (an increase of 223%). Ethylene, which was undetectable at the earliest stage, reached 466.32 mL kg^{-1} h^{-1} at Stage 6 (an increase of ≈20,811% relative to the first detectable level at Stage 3, 2.23 mL kg^{-1} h^{-1}). This slower progression promotes more uniform enzymatic activity and pigment transition, reducing the risk of quality defects such as uneven softening or surface spotting (Vu et al., 2019). Thus, natural ripening supports more synchronized peel-pulp maturation, ultimately yielding superior sensory and visual quality.

Softening is one of the most defining characteristics of fruit ripening, and in bananas, it serves as a significant determinant of consumer acceptance and marketability (Hoppu et al., 2021). In this study, both peel stiffness and flesh firmness declined significantly as ripening progressed ($p \leq 0.05$). Peel stiffness dropped from 54.01 ± 1.91 g s^{-1} (Stage 1) to 18.05 ± 0.45 g s^{-1} (Stage 7), representing a 66.57% decrease, while flesh firmness fell more drastically, from 178.88 ± 4.83 gf (Stage 1) to 36.84 ± 3.07 gf (Stage 7), amounting to a 79.39% reduction (Table 3).

These declines occurred progressively from Stage 1 through Stage 7, with the steepest reduction observed after Stage 4, consistent with the onset of massive cell wall disassembly. This softening process reflects extensive modifications and well-regulated enzymatic breakdown of cell wall polysaccharides (Tartaglia et al., 2021). The middle lamella is gradually dissolved by hydrolytic enzymes such as pectin methylesterase

(PME) and polygalacturonase (PG) (Verma et al., 2015). PME demethylates pectin, allowing PG to hydrolyze the now-accessible polygalacturonic acid chains (Illera et al., 2018). The resulting loss of pectic integrity reduces intercellular adhesion, leading to tissue collapse under mechanical pressure. Interestingly, flesh firmness declined more rapidly than peel stiffness throughout ripening, especially from Stage 4 onward (Table 3).

This suggests that cell wall disassembly occurs earlier and more extensively in the pulp. Tissue-specific sensitivity to ethylene and enzymatic activity, such as PME and PG, drives progressive pectin solubilization and cell wall degradation across ripening stages. Fruits exposed to exogenous ethylene soften faster than those undergoing natural ripening (Liu et al., 2015). Muthal et al. (2019) reported that flesh firmness in ethylene-treated bananas (*Musa acuminata* var. Poovan) decreased by over 60% within 48 hours. While this may accelerate shelf readiness, it often causes textural imbalance, such as softened pulp paired with incompletely colored peel, or even internal browning.

Pearson correlation analysis was conducted between respiration rate, ethylene production, peel color attributes (L^*, a^*, b^*, C^*, °hue), and texture parameters (peel stiffness and flesh firmness). Several strong and statistically significant correlations ($p \leq 0.05$) were observed (Figure 3). Figure 3 shows that the most notable was the strong positive correlation between CO_2 production and color parameters, particularly a^* ($r = 0.87$, $p \leq 0.05$), b^* ($r = 0.93$, $p \leq 0.05$), and °hue ($r = 0.90$, $p \leq 0.05$).

This suggests that, as respiration intensifies, there is a concurrent acceleration in chlorophyll breakdown and carotenoid expression. This is due to increased respiration, which supplies ATP and reduces equivalents (e.g., NADH/NADPH), which are essential for biosynthetic pathways, including pigment metabolism (Mendoza et al., 2016). Moreover, respiration is tightly linked to ethylene biosynthesis via the methionine cycle, further connecting it to pigment degradation and expression (Hu et al., 2021). Otherwise, ethylene production correlated negatively with both peel stiffness ($r = -0.62$, $p \leq 0.05$) and flesh firmness ($r = -0.65$, $p \leq 0.05$). This finding reflects ethylene's central role in regulating softening by activating cell wall-degrading enzymes such as PME, PG, and cellulases (Verma et al., 2015; Tipu & Sherif, 2024). A higher ethylene level initiates a cascade of gene expressions that disassemble the middle lamella and primary wall components, leading to measurable reductions in tissue firmness (Illera et al., 2018; Tartaglia et al., 2021).

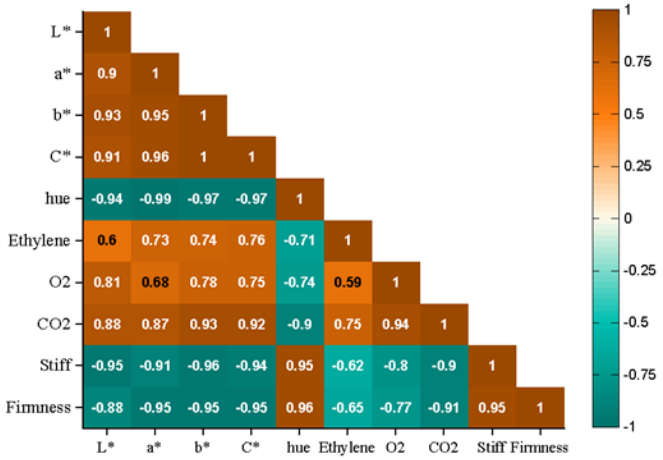

r = 0-0.19 (very weak), 0.20-0.39 (weak), 0.40-0.59 (moderate), 0.60-0.79 (strong), and 0.80-1.00 (very strong). All correlations shown are statistically significant at $p \leq 0.05$

Figure 3. Heatmap of Pearson correlation coefficients between physiological and quality parameters during ripening

Interestingly, CO_2 production showed a stronger correlation ($r = 0.75$-0.94, $p \leq 0.05$) with quality attributes than O_2 consumption ($r = 0.59$-0.81, $p \leq 0.05$), suggesting that the respiratory quotient or CO_2 evolution alone may serve as a more sensitive indicator of metabolic activity during ripening. Another strong correlation was observed between flesh firmness and a^* ($r = -0.95$, $p \leq 0.05$) and °hue ($r = 0.96$, $p \leq 0.05$), indicating that peel color, especially the °hue index, can be a non-destructive proxy for textural changes. Since color is easier and faster to measure, this relationship opens practical opportunities for developing automated ripening-monitoring tools (Paniagua et al., 2014; Ma et al., 2024). These correlations show that physiological factors, such as respiration and ethylene production, are closely linked to visible and tactile qualities of the fruit, rather than being separate processes. Understanding these relationships can guide postharvest handling decisions, such as optimal transport or marketing times, especially under non-ethylene-treated conditions.

Principal component analysis was used to identify key patterns and relationships among physiological and quality traits during Cavendish banana ripening (Figure 4). The first two components, PC1 and PC2, accounted for 92.94% of the total variance, with PC1 accounting for 87.69% and PC2 for 5.25%, indicating that this two-dimensional view effectively represents the main ripening dynamics. The loading vectors of quality and physiological parameters align with the typical climacteric ripening process. Parameters such as CO_2 production, ethylene emission, and peel color changes have strong positive loadings on PC1, emphasizing their essential roles in ripening. In contrast, peel stiffness, flesh firmness, and °hue load negatively, reflecting the expected decrease

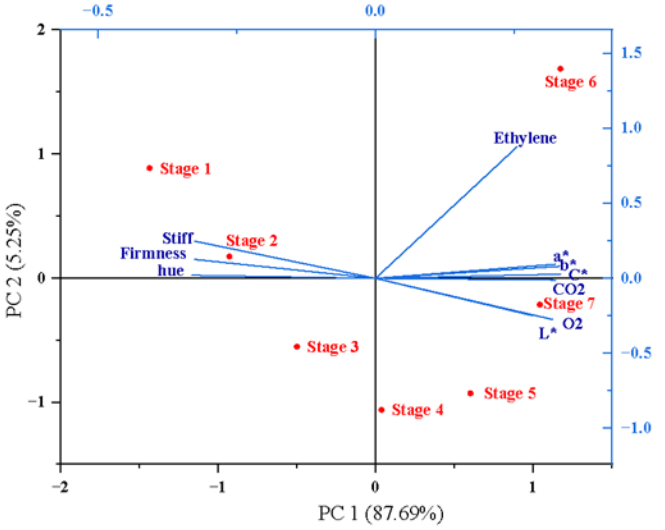

Figure 4. Principal Component Analysis between physiological and quality parameters during the ripening of Cavendish bananas

in tissue integrity as metabolic activity rises and reflecting chlorophyll degradation and carotenoid accumulation. This relationship highlights the parallel progression of tissue softening, respiration increase, and pigment development during ripening.

PC1 serves as the main axis distinguishing ripeness stages. Samples from Stages 1 and 2 cluster on the negative side of PC1, associated with firmness and peel stiffness, traits indicating intact cell walls. Conversely, Stages 6 and 7 are positioned on the positive side, corresponding with elevated ethylene production, respiration rates, and peel color changes (increases in a^*, b^*, and chroma). Stages 4 and 5 follow a relatively linear ripening pattern, and Stage 3 is distinct, located separately in the lower-left quadrant, away from CO_2, ethylene, and color vectors. This suggests it represents an early metabolic transition in the pre-climacteric phase, with metabolic changes beginning but without a full ethylene surge or clear visual ripening signs. Stage 7, though still associated with ethylene and respiration, clusters closer to the plot center, indicating a fully ripe or overripe state where physiological changes plateau and metabolic activity declines. Vector length and direction within the PCA highlight CO_2 production as the dominant factor influencing ripening dynamics. Its prominent, PC1-aligned vector suggests that changes in respiration rate are the strongest indicators distinguishing ripening stages.

The results of the calculations for the color and texture change rate constants over storage time are presented in Table 4. For color attributes (L^*, a^*, b^*, C^*, and ^{o}hue) and texture (peel stiffness and flesh firmness), the logistic model provided the best fit. This model produced high R^2 values (0.92-0.99) and relatively low RMSE values (1.12-28.83), indicating its strong ability to capture the nonlinear progression of ripening.

The L^* value has the lowest reaction constant (k = 0.25). The highest reaction constant (k) was observed in the firmness of fruit flesh (k = 1.72), indicating that texture degradation progresses more rapidly than external color transformation. Among the color parameters, the a^* value showed the greatest rate of change, reflecting the transition from green to yellow. A higher k value indicates a faster rate of quality change, whereas a lower k value indicates a slower rate (Lestari et al., 2020; Ningrum et al., 2023).

The logistic model provided valuable insights into the dynamic ripening behavior of Cavendish bananas, particularly by estimating the midpoint time (t_0), which marks the point at which 50% of the total change in a given attribute has occurred. Analysis of t_0 across color and texture parameters revealed distinct temporal patterns that mirror underlying physiological events during ripening. For peel color, the earliest transitions were observed in b^* (yellow-blue axis; t_0 = 4.90 days), chroma (C^*; t_0 = 5.23 days), and hue angle (hue°; t_0 = 5.23 days). These early shifts indicate that carotenoid accumulation, particularly lutein and β-carotene, commenced soon after harvest and became visually apparent by the fifth day (Kapoor et al., 2022). The a^* parameter (red-green axis; t_0 = 5.56 days) also shifted at an early stage, consistent with chlorophyll degradation, which reduces green pigmentation and allows carotenoids to dominate (Hu et al., 2021). In contrast, lightness (L^*) exhibited a later midpoint change (t_0 = 9.24 days), suggesting that the overall brightening of the peel surface occurs at a more advanced stage of ripening, after chlorophyll breakdown and carotenoid accumulation are well established. This sequence highlights that hue angle, b^*, and chroma are more sensitive indicators of the onset of ripening than lightness, which reflects the final visual manifestation of fruit maturity.

Textural parameters showed midpoint changes slightly earlier than color attributes. Peel stiffness decreased sharply with a t_0 of 3.95 days, while pulp firmness followed closely with a t_0 of 4.85 days. These results demonstrate that softening, particularly in the peel, is one of the earliest physiological events during natural ripening. The timing aligns with

Table 4. Estimated regression coefficients of time-based kinetic models describing the physical parameters of Cavendish bananas during natural ripening

Models	Parameters	Co/Uo	k	U	t_0	R^2	RMSE
Zero order	L^*	52.17	1.99			0.80	3.24
	a^*	-12.37	2.03			0.86	2.68
	b^*	32.44	1.90			0.90	2.13
	C^*	33.75	1.79			0.90	1.94
	^{o}hue	109.13	-0.84			0.87	19.00
	Stiffness	350.75	-27.22			0.80	44.22
	Firmness	752.49	-62.55			0.85	85.66
First order	L^*	53.26	-0.03			0.76	3.57
	a^*	-12.79	0.36			0.51	5.05
	b^*	33.58	-0.04			0.86	2.45
	C^*	34.67	-0.04			0.88	2.15
	^{o}hue	110.18	0.032			0.89	3.49
	Stiffness	393.54	0.14			0.89	32.88
	Firmness	803.58	0.13			0.83	91.57
Logistic	L^*	-199.25	0.25	271.15	9.24	0.95	1.62
	a^*	8.12	1.59	-17.82	5.56	0.98	1.12
	b^*	32.31	0.74	19.30	4.90	0.97	1.36
	C^*	34.51	0.82	17.60	5.23	0.96	1.23
	^{o}hue	80.30	-1.21	26.44	5.23	0.96	2.14
	Stiffness	95.76	-0.71	291.76	3.95	0.92	28.83
	Firmness	191.06	-1.72	525.08	4.85	0.99	26.64

C_0 - Initial value (Zero/First-order); U_0 - Initial value (Logistic); k - Rate constant; U - Maximum change value (Logistic); t_0 - Midpoint time when the rate of change is maximal (Logistic); R^2 - Coefficient of determination; RMSE - Root mean square error. The negative sign associated with k indicates that the reaction rate follows a declining trend. For clarity, only the absolute values are reported in the text.

extensive modifications in cell wall polysaccharides, including the solubilization of pectin and hemicellulose, which weaken cell-to-cell adhesion and reduce tissue rigidity (Shi et al., 2022).

Kinetic changes in color transformation (Figures 5 and 6) and texture degradation (Figure 7) during the ripening of Cavendish bananas followed similar patterns. This sigmoidal pattern that the model describes aligns well with the biological processes of fruit ripening. A trend also reported in other climacteric fruits, such as mango and tomato, indicates that logistic-type functions are reliable descriptors of color and texture dynamics (Nambi et al., 2016; Mai & Pathare, 2021). The use of kinetic models provides clear advantages, as they allow quantitative estimation of reaction rates, prediction of shelf-life, and comparison across studies. Slow changes in the early stages, rapid shifts during the climacteric phase, and stabilization toward the end of the process.

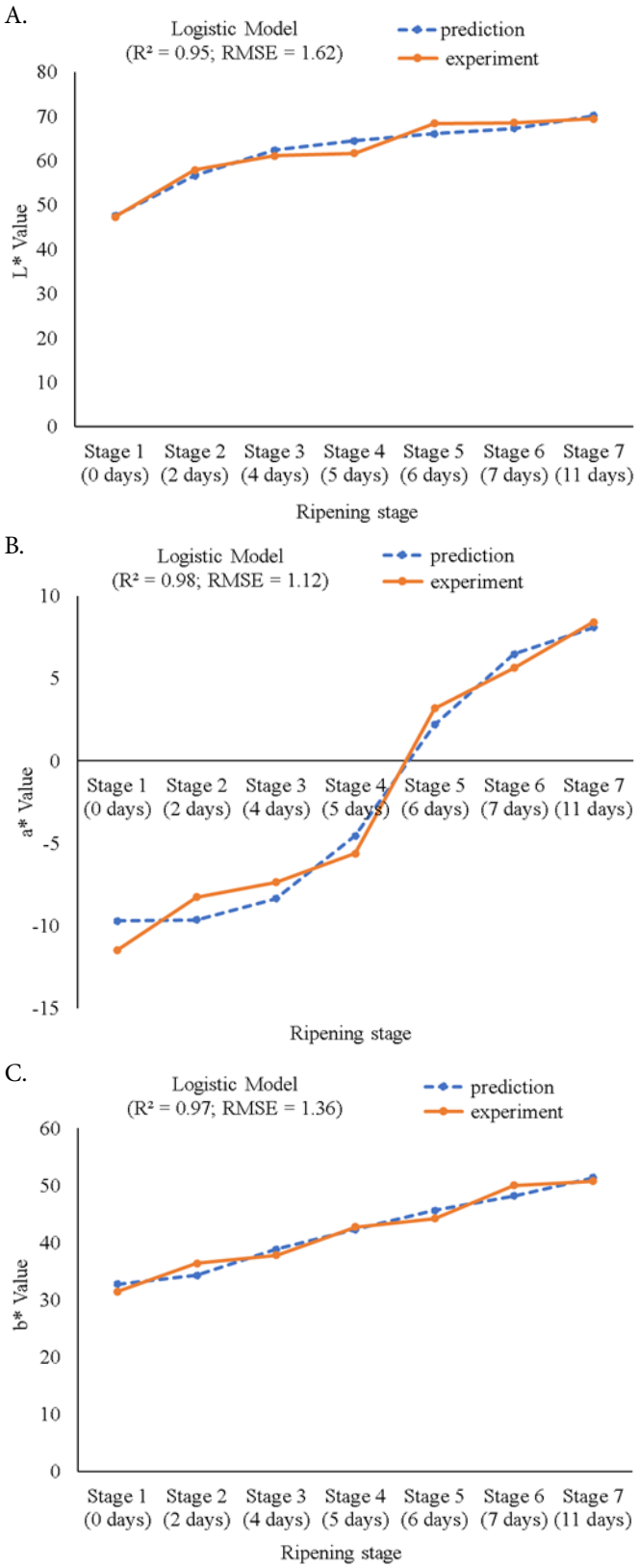

Figure 5. Comparison of predicted and experimental values using the Logistic model for L* value (A), a* value (B), and b* value (C) of Cavendish bananas during natural ripening

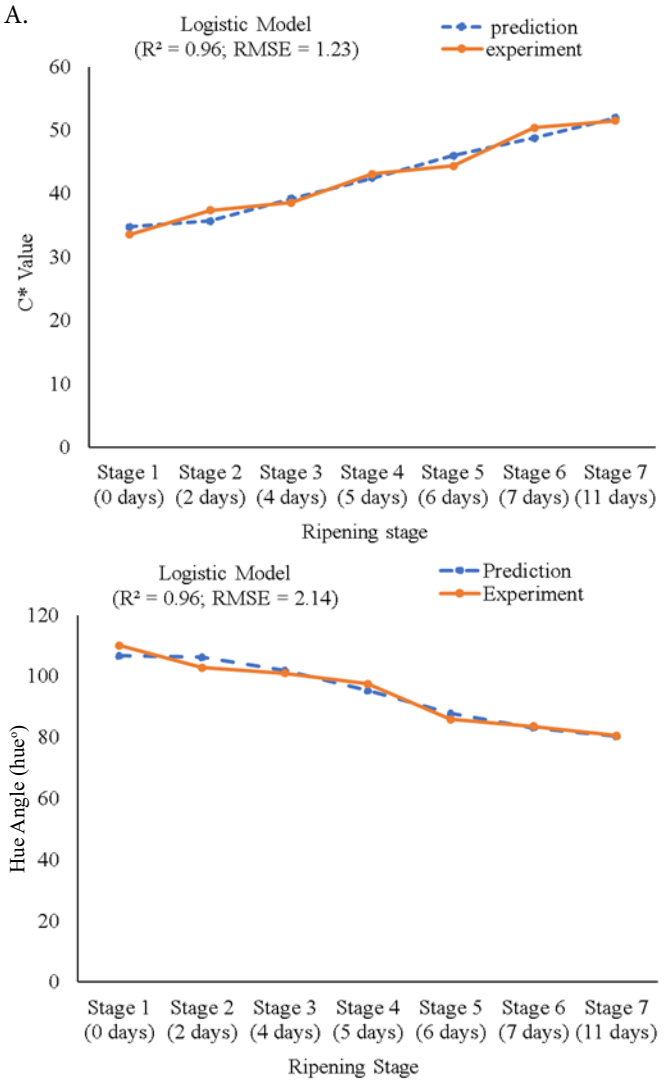

Figure 6. Comparison of predicted and experimental values using the Logistic model for C* value (A), and Hue angle (B) of Cavendish bananas during natural ripening

The natural ripening of Cavendish bananas ensures a gradual, physiologically balanced transformation of key quality attributes, such as peel color and flesh texture. This gradual change reflects the fruit's metabolic development and meets consumer expectations for ripeness, edibility, and freshness, which are key factors for optimal taste and digestibility (Hailu & Bekele, 2024). From a nutritional standpoint, this unforced progression may help preserve intrinsic quality, reducing the risks associated with premature or uneven ripening often caused by artificial interventions. Within this context, the kinetic analysis of physiological and quality attributes provides valuable insights for improving postharvest handling without

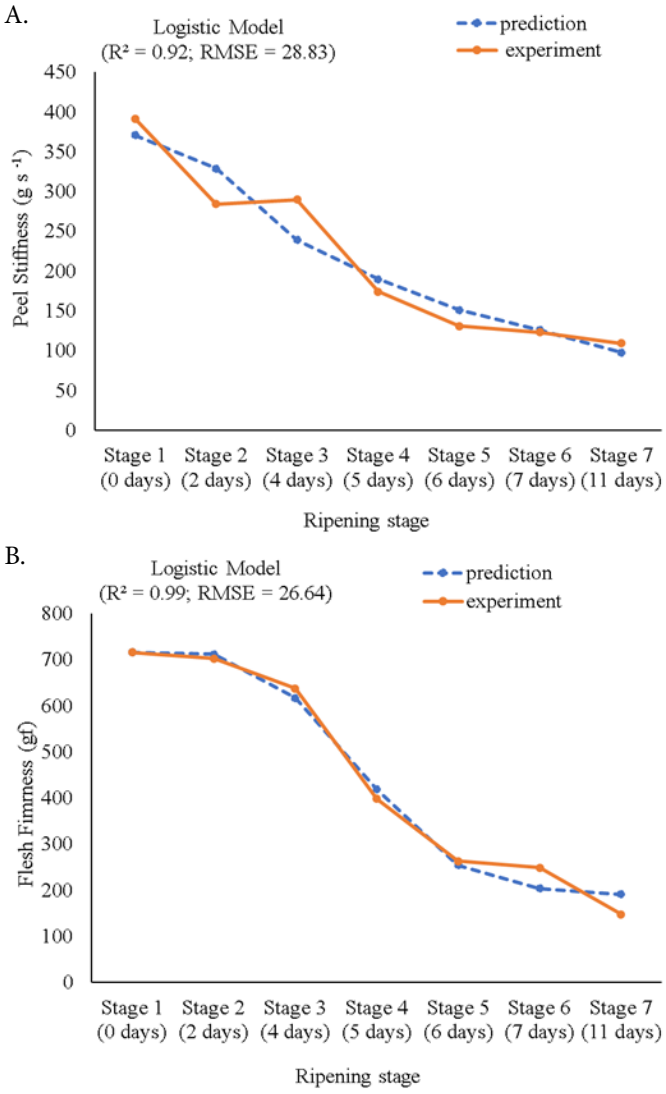

Figure 7. Comparison of predicted and experimental values using the Logistic model for peel stiffness (A), and flesh firmness (B) of Cavendish bananas during natural ripening

the need for external ripening agents. The logistic model provided a robust fit for predicting changes in peel color and texture, two key markers of ripeness and market readiness under ambient conditions (Figures 5-7).

The best models for respiration and ethylene production, which follow enzyme-like kinetics, the Michaelis-Menten model without inhibition, also performed excellently (Table 5). The high R^2 values (0.96-0.98) and low RMSE (0.002-30.48) confirmed that these processes are driven by enzyme-limited reactions and substrate availability (Table 5). The derived Michaelis-Menten constants (K_m) provide mechanistic insight, as the low and comparable values for O_2 consumption (4.74) and CO_2 production (4.97) reflect a high enzymatic affinity for oxygen, thereby ensuring efficient respiration.

In contrast, the significantly higher K_m for ethylene production (16.33) suggests a lower substrate affinity, implying that a threshold concentration of precursors must accumulate before the autocatalytic burst is triggered. Respiration rates and ethylene production in ripening Cavendish bananas are shown in Figure 8. This is consistent with the established understanding that enzymes like ACC synthase and AC Oxidase are central to ethylene biosynthesis during ripening (Tipu & Sherif, 2024). Interestingly, including inhibition models (whether competitive or noncompetitive) did not improve the model fit. This suggests that, in natural ripening conditions, CO_2 does not act as a feedback inhibitor for ethylene production or respiration. This finding contrasts with modified atmosphere storage systems, where high CO_2 levels can reduce ethylene synthesis and slow ripening (Badillo & Segura-Ponce, 2020).

In such controlled environments, elevated CO_2 concentrations are known to interfere with ethylene signaling pathways, delaying the onset of the climacteric phase and extending fruit shelf life (Alonso-Salinas et al., 2024). Simultaneously, the Michaelis-Menten model

Table 5. Parameters of the Michaelis-Menten equations used to estimate the respiration and ethylene production rates of Cavendish bananas during natural ripening

Michaelis-Menten Models	Parameters	Maximum rate (v_m) (mL kg^{-1} h^{-1})	Michaelis-Menten constant (k_m)	Inhibition constant			Validation models	
				k_c	k_u	k_n	R^2	RMSE
Normal (without inhibition)	O_2 consumption	0.006	4.74				0.98	0.002
	CO_2 production	0.008	4.97				0.98	0.006
	Ethylene production	3.06	16.33				0.96	30.48
Inhibition-competitive	O_2 consumption	58.30	58.36	1762.93			0.97	0.002
	CO_2 production	51.59	51.59	799.94			0.99	0.003
	Ethylene production	2763.32	106.96	-0.53			0.23	1136.26
Inhibition-uncompetitive	O_2 consumption	18.39	44744.37		8830		0.96	0.200
	CO_2 production	-0.82	604.17		8994.86		0.99	0.004
	Ethylene production	4153.50	140.01		-2.503		0.24	1299.65
Inhibition-noncompetitive	O_2 consumption	0.006	4.34			136.97	0.98	0.003
	CO_2 production	0.001	0.46			0.99	0.99	0.008
	Ethylene production	262.34	1.68			-76.52	0.259	137.20

v_m - Maximum reaction rate; k_m - Michaelis-Menten constant (substrate concentration at half of v_m); $k_c/k_u/k_n$ - Inhibition constant; R^2 - Coefficient of determination; RMSE - Root mean square error

without inhibition accurately described the natural patterns of respiration and ethylene production (Figure 8), underscoring its importance for monitoring the physiological progression of bananas during natural ripening. Together, these findings reinforce the value of natural ripening not only for promoting sensory and nutritional integrity but also for informing practical, low-cost, and non-invasive monitoring tools. Such tools can be particularly beneficial for smallholder supply chains in regions lacking cold storage and artificial ripening infrastructure, as they enable more precise shelf-life estimation, minimize postharvest losses, and improve harvest scheduling and local distribution efficiency.

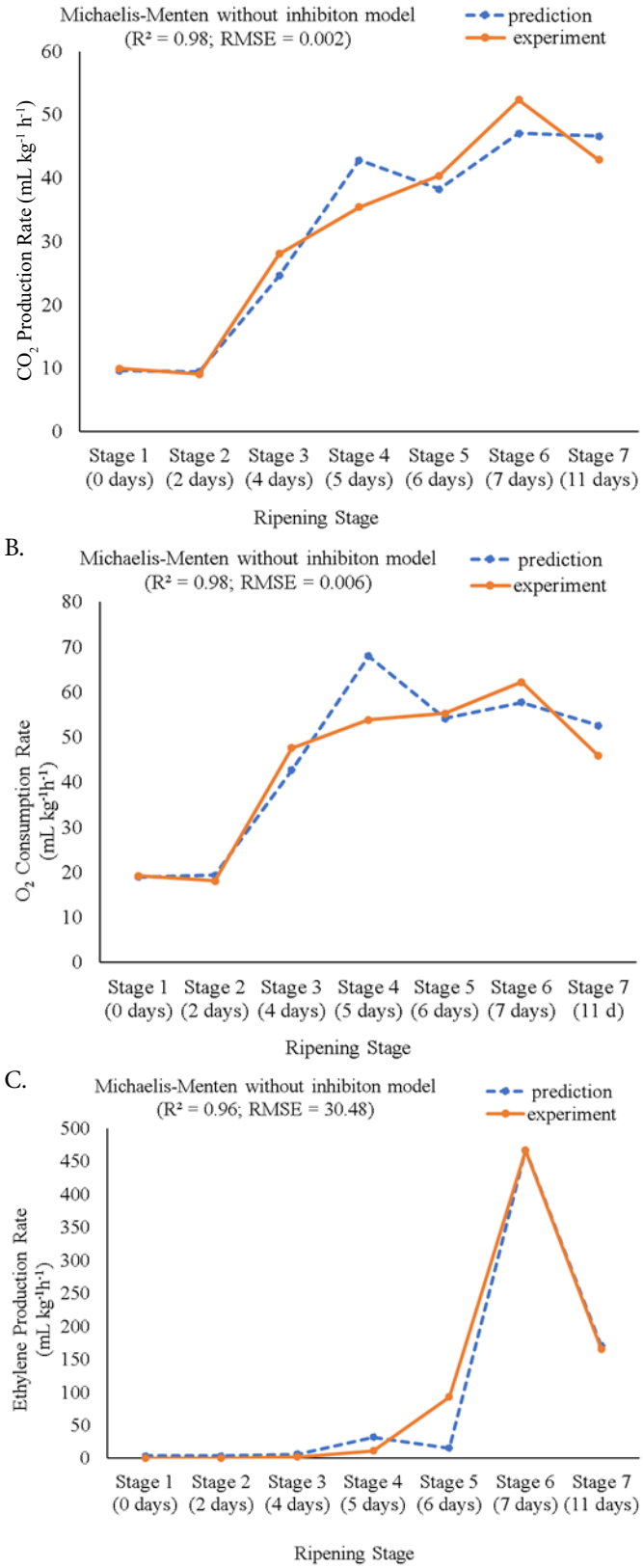

Figure 8. Comparison of predicted and experimental values using the Michaelis-Menten model for CO_2 production (A), O_2 consumption (B), and ethylene production (C) in Cavendish bananas during natural ripening

Conclusions

1. Respiration rate (CO_2 production) emerged as the most reliable and practical indicator for monitoring the natural ripening of Cavendish bananas, showing the strongest correlation with peel color transition and flesh softening.

2. A critical insight for quality management is that texture degradation precedes visible peel degreening. This indicates that internal biochemical changes are already advanced before external color cues become reliable, underscoring the limitation of relying solely on visual color as a ripeness index.

3. Kinetic analysis confirmed that the logistic model accurately describes the sigmoidal dynamics of color and texture. In contrast, the Michaelis-Menten model (without inhibition) effectively captures the enzymatic kinetics of respiration and ethylene production. Together, these models provide a robust predictive framework for characterizing natural ripening.

4. Overall, these findings offer practical tools for postharvest optimization. CO_2 monitoring shows strong potential as a non-destructive indicator for industry. At the same time, the synchronized progression of natural ripening supports its preference over artificial methods for achieving balanced and superior fruit quality.

Contribution of authors: Rima Kumalasari: conceptualization, methodology, investigation, data curation, formal analysis, and writing of the original draft. Andriati Ningrum: investigation, validation, visualization, and manuscript review and editing. Achmat Sarifudin: resources, supervision, and critical review of the manuscript. Djagal Wiseso Marseno: conceptualization, project administration, supervision, and overall coordination of the research activities.

Data availability statement: The authors declare that there are no data underlying the text.

Conflict of interest: The authors declare no conflicts of interest.

Financing statement: This research was funded by the Badan Riset dan Inovasi Nasional, BRIN (National Research and Innovation Agency) of Indonesia under Grant No. 9/III.11/HK/2023.

Acknowledgment: The authors gratefully acknowledge the Badan Riset dan Inovasi Nasional (BRIN, National Research and Innovation Agency) of Indonesia for funding and supporting this research. The authors also thank the laboratory

staff and all individuals who contributed to the experimental and analytical work during the study.

Literature Cited

Acevedo, S. A.; Díaz Carrillo, Á. J.; Flórez-López, E.; Grande-Tovar, C. D. Recovery of banana waste-loss from production and processing: A contribution to a circular economy. Molecules, v.26, e5282, 2021. https://doi.org/10.3390/molecules26175282

Alonso-Salinas, R.; López-Miranda, S.; Pérez-López, A. J.; Acosta-Motos, J. R. Strategies to delay ethylene-mediated ripening in climacteric fruits: Implications for shelf life extension and postharvest quality. Horticulturae, v.10, e840, 2024. https://doi.org/10.3390/horticulturae10080840.

Badillo, G. M.; Segura-Ponce, L. A. Classic and reaction-diffusion models used in modified atmosphere packaging (MAP) of fruit and vegetables. Food Engineering Reviews, v.12, p.209-228, 2020. https://doi.org/10.1007/s12393-020-09214-3

Cordenunsi-Lysenko, B. R.; Nascimento, J. R. O.; Castro-Alves, V. C.; Purgatto, E.; Fabi, J. P.; Peroni-Okyta, F. H. G. The starch is (not) just another brick in the wall: the primary metabolism of sugars during banana ripening. Frontiers in Plant Science, v.10, e391, 2019. https://doi.org/10.3389/fpls.2019.00391.

Hailu, W.; Bekele, T. Quality and phsio-chemical changes associated with processing and properties of fruits and vegetables. Cogent Food & Agriculture, v.10, e2419957, 2024. https://doi.org/10.1080/23311932.2024.2419957

Hoppu, U.; Puputti, S.; Sandell, M. Factors related to sensory properties and consumer acceptance of vegetables. Critical Reviews in Food Science and Nutrition, v. 61, p.1751-1761, 2021. https://doi.org/10.1080/10408398.2020.1767034

Hu, X.; Khan, I.; Jiao, Q.; Zada, A.; Jia, T. Chlorophyllase, a common plant hydrolase enzyme with a long history, is still a puzzle. Genes, v.12, e1871, 2021. https://doi.org/10.3390/genes12121871

Illera, A. E.; Sanz Díez, M.; Trigueros Andrés, E.; Beltrán Calvo, S.; Gómez, R. M. Effect of high pressure carbon dioxide on tomato juice: inactivation kinetics of pectin methylesterase and polygalacturonase and determination of other quality parameters. Journal of Food Engineering. v.239, p.64-71, 2018. https://doi.org/10.1016/j.jfoodeng.2018.06.027

Kapoor, L.; Simkin, A. J.; Doss, C. G. P; Siva, R. Fruit ripening: dynamics and integrated analysis of carotenoids and anthocyanins. BMC Plant Biology, v. 22, e27, 2022. https://doi.org/10.1186/s12870-021-03411-w.

Kaur, J.; Singh, Z.; Mazhar, M. S.; Shah, H. M. S.; Woodward, A. Changes in physical attributes, activities of fruit softening enzymes, cell wall polysaccharides and fruit quality of jackfruit (*Artocarpus heterophyllus* Lam.) as influenced by maturation and ripening. Horticulturae, v.10, e1264, 2024. https://doi.org/10.3390/horticulturae10121264.

Lestari, H. A.; Prabowo, A. A. P.; Soolany, C. Kinetic analysis of physical quality change on eggplant (*Solanum melongena* L.) during storage. Journal Agritechno, v.13, p.84-89, 2020. https://doi.org/10.20956/at.v13i2.339.

Liu, M.; Julien, P.; Christian, C.; Jean-Paul, R.; Mondher, B. Ethylene control of fruit ripening: revisiting the complex network of transcriptional regulation. Plant Physiology, v.169, p.2380-2390, 2015. https://doi.org/10.1104/pp.15.01361.

Ma, J.; Li, M.; Fan, W.; Liu, J. State-of-the-art techniques for fruit maturity detection. Agronomy, v.14, e2783, 2024. https://doi.org/10.3390/agronomy14122783.

Mai, A. D.; Pathare, P. B. Kinetic modeling of quality changes of tomato during storage. Agricultural Engineering International: CIGR Journal, v.23, p.183-193, 2021. https://doi.org/10.1111/jfpe.13808

Mangaraj, S.; Goswami, T. K. Measurement and modeling of respiration rate of guava (cv. Baruipur) for modified atmosphere packaging. International Journal of Food Properties, v.14, p.609-628, 2011. https://doi.org/10.1080/10942910903312403.

Mendoza, R.; Castellanos, D. A.; García, J. C.; Vargas, J. C.; Herrera, A. O. Ethylene production, respiration and gas exchange modelling in modified atmosphere packaging for banana fruits. International Journal of Food Science & Technology, v.51, p.777-788, 2016. https://doi.org/10.1111/ijfs.13037.

Müller, T.; Kräutler, B. Chlorophyll breakdown as seen in bananas: sign of aging and ripening - a mini-review. Gerontology, v.57, p.521-527, 2011. https://doi.org/10.1159/000321877.

Muthal, T.; Harini, R.; Sunil, C.; Chidanand, D. Effect of artificial ripening techniques on physico-chemical properties of banana (*Musa* sp) variety Poovan. International Journal of Pure and Applied Bioscience, v.7, p.482-489, 2019. https://doi.org/10.18782/2320-7051.7453

Nambi, V. E.; Thangavel, K.; Shahir, S.; Chandrasekar, V. Color kinetics during ripening of Indian mangoes. International Journal of Food Properties, v.19, p.2147-2155, 2016. https://doi.org/10.1080/10942912.2015.1089281.

Ningrum, L.; Warsiki, E.; Purwanto, Y. A.; Widayanti, S. M. Kinetic model of quality changes in Arumanis mango (*Mangifera indic*a L.) during the supply chain. Agrointek: Jurnal Teknologi Industri Pertanian, v.17, p.813-820, 2023. https://doi.org/10.21107/agrointek.v17i4.17415.

Paniagua, C.; Posé, S.; Morris, V. J.; Kirby, A. R.; Quesada, M. A.; Mercado, J. A. Fruit softening and pectin disassembly: an overview of nanostructural pectin modifications assessed by atomic force microscopy. Annals of Botany, v.114, p.1375-1383, 2014. https://doi.org/10.1093/aob/mcu149 .

Salaemae, N.; Pongprasert, N.; Phornvillay, S.; Kaewsuksaeng, S.; Shigyo, M.; Ito, S.; Yamauchi, N.; Srilaong, V. Impact of electrostatic atomized water particles treatment on chlorophyll degradation and delay ripening in a thai banana (*Musa* × *paradisiaca*, cv.'Namwa'Banana) during storage. The Horticulture Journal, v.93, p.23-32, 2024. https://doi.org/10.2503/hortj.qh-096.

Scott, G. J. A review of root, tuber and banana crops in developing countries: past, present and future. International Journal of Food Science and Technology, v.56, p.1093-1114, 2021. https://doi.org/10.1111/ijfs.14778

Shi, Y.; Li, B. J.; Su, G.; Zhang, M.; Grierson, D.; Chen, K. S. Transcriptional regulation of fleshy fruit texture. Journal of Integrative Plant Biology, v.64, p.1649-1672, 2022. https://doi.org/10.1111/jipb.13316.

Sugianti, C.; Imaizumi, T.; Thammawong, M.; Nakano, K. Recent postharvest technologies in the banana supply chain. Reviews in Agricultural Science, v.10, p.123-137, 2022. https://doi.org/10.7831/ras.10.0_123

Tanaka, A.; Ito, H. Chlorophyll degradation and its physiological function. Plant and Cell Physiology, v.66, p.139-152, 2025. https://doi.org/10.1093/pcp/pcae093

Tartaglia, M.; Sciarrillo, R.; Zuzolo, D.; Amoresano, A.; Illiano, A.; Pinto, G.; Jorrín-Novo, J. V.; Guarino, C. Why consumers prefer green friariello pepper: changes in the protein and metabolite profiles along the ripening. Frontiers in Plant Science, v.12, e668562, 2021. https://doi.org/10.3389/fpls.2021.668562

Tipu, M. M.; Sherif, S. M. Ethylene and its crosstalk with hormonal pathways in fruit ripening: mechanisms, modulation, and commercial exploitation. Frontiers in Plant Science, v.15, e1475496, 2024. https://doi.org/10.3389/fpls.2024.1475496.

Tuly, S. S.; Mahiuddin, M.; Karim, A. Mathematical modeling of nutritional, color, texture, and microbial activity changes in fruit and vegetables during drying: A critical review. Critical Reviews in Food Science and Nutrition, v.63, p.1877-1900, 2023. https://doi.org/10.1080/10408398.2021.1969533

Verma, C.; Singh, R.; Singh, R. B.; Mishra, S. Biochemical and in-silico studies on pectin methylesterase from G9 variety of *Musa acuminata* for delayed ripening. The Open Biochemistry Journal, v.9, e15, 2015. https://doi.org/10.2174/1874091x01509010015.

Vu, H. T.; Scarlett, C. J.; Vuong, Q. V. Changes of phytochemicals and antioxidant capacity of banana peel during the ripening process; with and without ethylene treatment. Scientia Horticulturae, v.253, p.255-262, 2019. https://doi.org/10.1016/j.scienta.2019.04.043.

Xu, Y.; Liu, S. Botanical-based simulation of color change in fruit ripening: Taking tomato as an example. Computer Animation and Virtual Worlds, v.35, e2225, 2024. https://doi.org/10.1002/cav.2225